

Comparison of Simultaneous and Sequential Two-View Registration for 3D/2D Registration of Vascular Images

Chetna Pathak¹, Mark Van Horn¹, Susan Weeks², Elizabeth Bullitt¹

¹Department of Surgery, University of North Carolina, Chapel Hill, NC
{cpathak, mark_vanhorn, bullitt} @med.unc.edu
<http://casilab.med.unc.edu/>

²Department of Radiology, University of North Carolina, Chapel Hill, NC
sue_weeks@med.unc.edu

Abstract. Accurate 3D/2D vessel registration is complicated by issues of image quality, occlusion, and other problems. This study performs a quantitative comparison of 3D/2D vessel registration in which vessels segmented from preoperative CT or MR are registered with biplane x-ray angiograms by either a) simultaneous two-view registration with advance calculation of the relative pose of the two views, or b) sequential registration with each view. We conclude on the basis of phantom studies that, even in the absence of image errors, simultaneous two-view registration is more accurate than sequential registration. In more complex settings, including clinical conditions, the relative accuracy of simultaneous two-view registration is even greater.

1. Introduction

The objective of 3D/2D registration is to align spatial data to projective data. Given a 3D model and its 2D projection, 3D/2D registration determines the pose (orientation and position) of the model at which its 2D image was taken. This paper discusses the registration of 3D vessels, segmented preoperatively from computed tomographic (CT) or magnetic resonance (MR) images, to biplane, x-ray angiograms.

The driving clinical problem is the Transjugular Intrahepatic Portosystemic Shunt (TIPS) procedure, which creates a channel between the portal and hepatic veins [1]. We are currently developing an image-guided system for this procedure. One of the major challenges has been achieving accurate 3D/2D registration under conditions in which the x-ray angiograms are noisy and contain severe projection overlap.

Several groups have described effective methods of 3D/2D vascular registration [2,3,4,5]. The purpose of the current paper is not to evaluate a specific registration metric, but rather to compare the efficacy of simultaneous, two-view registration with sequential registration. This issue has received little attention, although one paper notes in passing that simultaneous, two-view registration appears more effective than single-view registration [6]. However, no quantitative assessment or detailed analysis was provided.

The current study uses both phantom and clinical data to evaluate the performance of registration of a presegmented, 3D vessel model to biplane fluoroscopic images under two conditions. In the first, the relationship between the cameras capturing the two views is determined in advance and registration of the 3D model to the two views is carried out simultaneously. In the second case, the 3D model is registered sequentially and independently to each view.

We conclude that the simultaneous approach is more accurate than the sequential approach even under ideal conditions. In the presence of image errors, the difference between the performance of the two methods increases. Although this report employs a particular registration metric, the findings in regard to sequential/simultaneous view registration should be applicable to 3D/2D registration methods using other metrics.

2. Methods

2.1 Phantom studies

The purpose of the phantom studies was to evaluate registration accuracy under conditions in which ground truth is known and under varying conditions of image quality. All studies were performed in blinded fashion, with the individual performing the registration unaware of the 3D pose of the vessels until after study completion.

Simulated angiograms were created by generating projections of four different portal venous trees, each segmented from the CT or MR of a different patient, and each containing 7-15 vessels. The fields of view ranged from 9° to 16.5° , and the relative angle between the two views ranged from 80° to 90° , with arbitrary placement and rotation of the 3D model within the imaged field. Two sets of pseudoangiogram pairs were generated for each of the four vascular models, each using different model poses and different combinations of camera intrinsics. For each 3D vessel point, a circle was projected upon the view-plane whose radius was calculated on the basis of the 3D vessel radius and the rules of projection geometry. By using a combination of buffers and by summing image intensities, images were generated that simulated angiographic images under conditions of vessel overlap (Fig. 1).

For sequential registration, the operator was given each view's camera intrinsics, and registration was performed individually for each image. For simultaneous view registration, the operator was given both the camera intrinsics and the relationship between the two views, and registration was performed on both views simultaneously. The initial estimate of 3D model pose was up to 16° off and up to 65 mm away from the actual position of the model used during synthetic image creation.

3D/2D registration was performed using a metric that optimizes a view-plane based disparity measure based on the iterative closest point algorithm between the 3D vessel skeletons and the skeletons of the vessel projections seen on angiograms [5].

Registration accuracy was measured by comparing the 3D location of each point in the 3D model following registration with the known location of each point during synthetic image generation. Mean 3D point placement errors were calculated for each

case during each study. One result was reported per case when simultaneous registration was employed, and two results were reported per case (one each for Anterior-Posterior (AP) and Lateral images) when sequential registrations were employed. Three different phantom studies were performed:

1) Ideal case pseudoangiograms: Registration of the 8 image pairs with their respective 3D models were evaluated under conditions of projection overlap, but without added noise and with perfect one-to-one correspondence between vessels of the 3D model and their projections on pseudoangiograms. Fig. 1 illustrates a perspective projection of the 3D model and its AP and lateral pseudoangiograms.

2) Noisy pseudoangiograms: This study was identical to the one above, but with Gaussian noise added to the pseudoangiograms. The addition of noise both obscures smaller vessels and can confuse the determination of vessel skeletons (Fig. 2).

3) Noisy pseudoangiograms without one-to-one vessel correspondence: This study was identical to the two above, but with the deletion of 3-8 branches from the 3D model. This situation provides a partial simulation of the actual clinical condition, in which a noisy x-ray angiogram can show vessels that the 3D model does not. Similarly, the 3D model may contain vessels that are not visible in the angiogram.

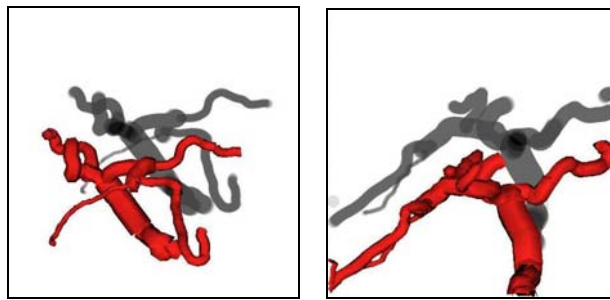


Fig. 1. An example of ideal-case simulated pseudoangiograms (gray), AP (left) and lateral (right). Also shown is a perspective projection of the 3D segmented vasculature (red)

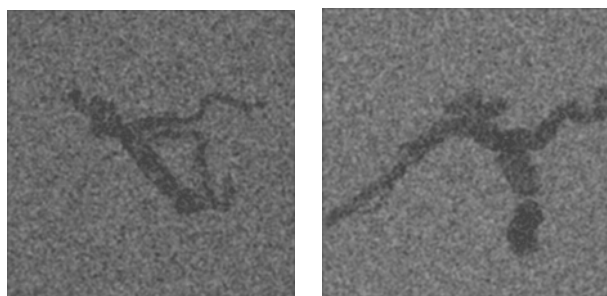


Fig. 2. Simulated angiograms with added noise. Vessels have the same pose as shown in Fig. 1

2.2 Clinical studies

Registration in the actual clinical setting contains additional sources of error. A comparison of simultaneous and sequential two-view registration was also performed with three clinical cases using AP and lateral angiographic images obtained during the TIPS procedure.



Fig. 3. AP (left) and lateral (right) abdominal angiograms obtained intra-operatively. Note the noisiness of the data and the significant projection overlap induced by wide-diameter vessels

Preoperative images of the 3D liver vasculature were obtained by CT or MR. For CT scans, a Siemens Somatom Plus system was used with collimation 0.56x0.56x2.5 mm. MR scans were obtained on a Siemens MagicVision 1.5T system with collimation 0.86x0.86x3 mm. The voxel size was variable, but in the range of 1.5x1.5x3 mm.

The portal venous tree was segmented from the 3D image data. Vessel extraction involved 3 steps: definition of a seed point, automatic extraction of an image intensity ridge representing the vessel's central skeleton, and automatic determination of vessel radius at each skeleton point [7]. Vessels are represented as sets of 4-dimensional points with an (x,y,z) spatial position and associated radius.

A Siemens Neurostar biplane digital angiographic unit was used to obtain x-ray angiograms as biplane views, separated by approximately 90 degrees. The field of view ranged from 8.7° to 16.5°. Images were captured and stored as 8-bit 884x884 pixel images. Fig. 3 shows sample clinical images.

For patient studies, the relationship between the two fluoroscopic views was calibrated using a Plexiglas phantom containing a known arrangement of 5 mm diameter metallic spheres. The projection matrix for each view was calculated by taking an x-ray image of the phantom and minimizing the distance between observed pixel coordinates and ideal projection of each control point [8]. Intrinsic camera parameters were also calculated for each view, using the same phantom.

Validation of registration results

The evaluation of clinical results is difficult since ground truth is unknown. Registration accuracy was estimated in these cases by reconstructing into 3D, a point

that could be identified in both AP and lateral views, and comparing the location of this reconstructed 3D point to that of its corresponding point in the 3D model following registration. One subject ('Patient 1' in Table 2) had a metal clip in the liver as a result of previous surgery, and this clip was visible in the preoperative CT and on both projection views. The same subject also had 2 vessel branch-points that, with the help of an expert radiologist, could be associated on the AP and lateral projection views. Patients 2 and 3 had 3 and 2 vessel branch-points, respectively, that could similarly be associated on the AP and lateral views.

3. Results

3.1 Phantom Studies

For each test case, registration errors are presented for ideal pseudoangiograms, noisy pseudoangiograms and noisy pseudoangiograms without one-to-one vessel correspondences. For each of these pseudoangiogram pairs, accuracy is reported for simultaneous, sequential AP, and sequential lateral registrations.

Addition of noise to the image obscures small vessels and distorts vessel shape, making an accurate registration harder. The lack of one-to-one vessel correspondence is another source of error. For example, the image on the left in Fig. 4 shows a trimmed 3D model registered with the pseudoangiogram. On the right the model is shown with all branches present. The green curves identify the position of previously deleted branches, thus highlighting the error.

The vessel registration errors for the phantom studies, presented in Tables 1 and 2 and in Figures 5, 6 and 7, are calculated as detailed in section 2.1.

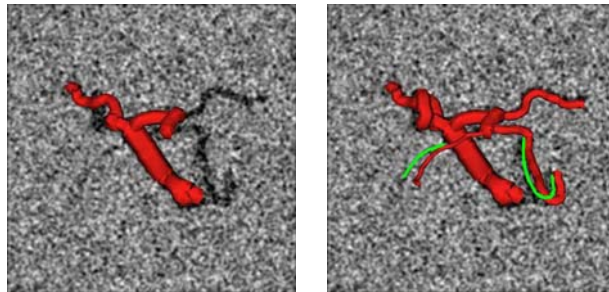


Fig. 4. Registration difficulties in presence of noise and without one-to-one correspondence

3.2 Clinical Studies

Table 3 contains the registration accuracy data for the clinical trials, calculated as detailed in section 2.4. For patient 1, the registration error given is the mean of the error over three points - a surgical clip and two vessel branch-points. For patients 2 and 3, the mean registration error for 3 and 2 branch-points, respectively, is presented.

Table 1. Registration errors for phantom studies for the ideal and noisy pseudoangiograms. Errors are in mm and are presented in the ‘mean (maximum)’ format

Case	Ideal pseudoangiograms			Noisy pseudoangiograms		
	Sequential Registration		Simultaneous Regn.	Sequential Registration		Simultaneous Regn.
	AP	Lateral		AP	Lateral	
1	1.1 (2.1)	1.1 (2.1)	0.3 (0.6)	4.3 (4.8)	0.7 (1.7)	0.5 (1.9)
2	3.1 (3.9)	1.1 (2.0)	0.3 (0.6)	2.1 (3.6)	1.1 (2.0)	0.7 (1.1)
3	1.0 (2.2)	0.3 (0.5)	0.3 (0.5)	1.4 (2.0)	5.0 (5.5)	0.9 (1.2)
4	2.8 (2.9)	3.7 (4.1)	0.7 (0.9)	6.3 (6.9)	1.3 (1.4)	1.0 (1.2)
5	3.1 (5.3)	1.1 (1.5)	0.2 (0.2)	1.7 (2.2)	1.7 (2.2)	1.1 (1.6)
6	4.1 (4.2)	3.8 (5.3)	0.2 (0.2)	2.0 (4.4)	1.9 (3.8)	1.0 (2.6)
7	0.6 (1.0)	0.6 (1.0)	0.2 (0.2)	8.2 (9.2)	3.4 (4.5)	1.1 (1.4)
8	0.5 (1.0)	1.0 (1.7)	0.4 (0.6)	2.3 (3.8)	4.9 (6.1)	0.6 (0.7)

Table 2. Phantom registration errors in mm for noisy pseudoangiograms without one-to-one correspondence

Case	Noisy pseudoangiograms without 1-to-1 correspondence		
	Sequential Registration		Simultaneous Registration
	AP	Lateral	
1	1.1 (2.9)	1.9 (2.2)	0.5 (1.1)
2	3.4 (5.5)	1.1 (2.0)	1.1 (2.3)
3	1.4 (4.5)	6.8 (7.0)	1.0 (1.4)
4	5.3 (7.4)	5.0 (6.9)	1.0 (1.5)
5	7.3 (8.2)	6.0 (6.9)	1.2 (2.0)
6	3.8 (5.4)	7.7 (8.7)	1.1 (2.9)
7	8.7 (9.3)	8.0 (8.8)	0.8 (1.4)
8	1.2 (1.9)	4.2 (6.8)	0.6 (0.9)

Table 3. Registration errors in mm for clinical trials. Errors are in ‘mean (maximum)’ format

Patient	Sequential Registration	Simultaneous Registrations
1	6.1 (7.2)	1.9 (2.12)
2	5.5 (9.6)	2.6 (3.7)
3	4.0 (4.8)	2.4 (2.5)

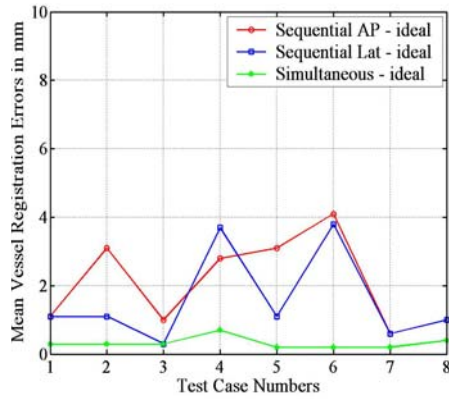


Fig. 5. Mean registration errors for the phantom studies with ideal angiograms

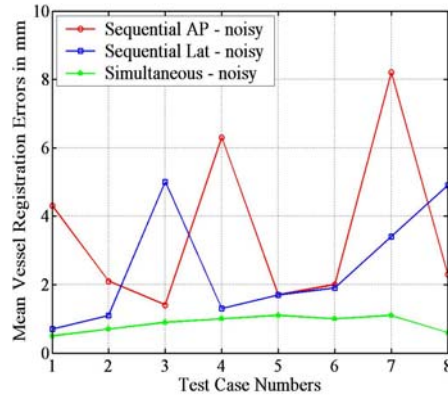


Fig. 6. Mean registration errors for the phantom studies with noisy angiograms

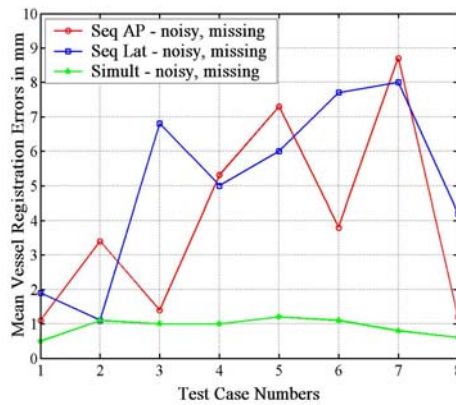


Fig. 7. Mean errors for phantom studies with noise and without one-to-one correspondence

4. Discussion and Conclusion

This paper compares the accuracy of simultaneous and sequential two-view registration in both phantom and clinical images of abnormal hepatic vasculature. The magnitude of the error we report for sequential-view registration is larger than the 1-2 mm error generally described in the literature [3,4,5]. Almost all prior studies evaluating 2D-3D vessel registration accuracy have used noiseless images, thin vessels, and one-to-one vessel correspondence, however. As shown by Figure 3, the images generated during TIPS are often of low quality and many vessels are thick - the main branch of the portal vein may be over 1 cm wide. Thick vessels increase projection overlap and complicate both centerline and branch-point definition. The difficulty of accurate 2D-3D registration is thus high in this actual clinical situation.

The current study details the behavior of the two registration methods with changes in image quality. Even under ideal conditions, one might expect simultaneous two-view registration to perform superiorly since with single-view registration, translation of an object along the depth axis produces relatively little change on projection. Simultaneous use of two orthogonal views allows each registration to correct the depth estimate of the other. Our phantom studies confirm this hypothesis, with improvement of accuracy by simultaneous registration even under ideal conditions.

The difference between the two approaches becomes more pronounced under conditions of noise and lack of one-to-one vessel correspondence—conditions evaluated both in our phantom studies and in clinical data. Indeed, in two of the three clinical cases, the error in simultaneous registration was more than twice the magnitude of the error for sequential registration. This finding may result from the ability of one view to compensate for regional ambiguities in the other.

We conclude that simultaneous, two-view registration produces significantly more accurate results than consecutive view registration. These findings should be applicable to a variety of 2D-3D registration metrics, and are of interest to those involved in the guidance of endovascular surgery.

References

1. J.M. LaBerge, E.J. Ring, R.L. Gordon, J.R. Lake, M.M. Doherty, K.A. Somber, J.P. Roberts, N.L. Ascher, "Creation of Transjugular Intrahepatic Portosystemic Shunts with the Wallstent Endoprosthesis: Results in 100 Patients", *Radiology*, 187(2):413-20, May 1993
2. J. Feldmar, G. Malandain, N. Ayache, S. Fernández-Vidal, E. Maurincombe and Y. Troussset, "Matching 3D MR Angiography Data and 2D X-ray Angiograms", *CVRMed-MRCAS 1997, Grenoble, France*, pp.129-138
3. H.M. Chan, A.C.S. Chung, S.C.H. Yu, W.M. Wells, "2D-3D Vascular Registration between Digital Subtraction Angiographic (DSA) and Magnetic Resonance Angiographic (MRA) Images", *IEEE International Symposium on Biomedical Imaging: From Nano to Macro, April 2004*
4. Y. Kita, D. Wilson, J.A. Noble "Real-time Registration of 3D Cerebral Vessels to X-ray Angiograms" *MICCAI 1997*, pp. 1125-1133
5. A. Liu, E. Bullitt, S. Pizer "3D/2D Registration via Skeletal Near Projective Invariance in Tubular Objects", *Medical Image Computing and Computer-Assisted Intervention, LNCS 1496: 952-963, MICCAI 1998*
6. Y. Kita, D. Wilson, J.A. Noble, N. Kita "A quick 3D-2D Registration Method for a Wide-Range of Applications", *Proceedings of the International Conference on Pattern Recognition*, pp. 981-986, *ICPR 2000*
7. Aylward S, Bullitt E : Initialization, noise, singularities and scale in height ridge traversal for tubular object centerline extraction. *IEEE-TMI* 21:61-75, 2002
8. O. Faugeras "Three-Dimensional Computer Vision: A Geometric Viewpoint", *MIT Press 1996*

Acknowledgements

This work was supported by R01 HL69808 NIH-HLB.